DOI: 10.1002/ejic.201000831

Synthesis and Crystal Structure of Novel Biheterometal and Triheterometal Alkoxide Clusters – Highly Active Catalysts for the Polymerization of ε-Caprolactone

Hongting Sheng,*[a,b] Yan Feng,[a] Yong Zhang,[b] and Qi Shen*[b]

Keywords: Heterometal clusters / Lanthanides / Alkali metals / Alkoxide / Polymerization / ε-Caprolactone

The effect of the alkali metal on the synthesis, crystal structure, and catalytic reactivity of lanthanide–alkali metal alkoxide clusters is reported. Anhydrous $LnCl_3$ reacts with 6.5 equiv. of $KOCH_2CH_2N(CH_3)_2$ and 1.5 equiv. of KOH in tetrahydrofuran (THF) to give the corresponding lanthanide–potassium biheterometal alkoxide clusters $[Ln_4K_{20}(OCH_2CH_2NMe_2)_{26}(OH)_6]$ [Ln = Nd (**1**), Pr (**2**), Yb (**3**)] in high yield. Anhydrous $YbCl_3$ reacts with $KOCH_2CH_2N(CH_3)_2$ and NaOH with different molar ratios of 1:9:3 and 1:9:4 to afford the lanthanide–potassium–sodium triheterometal alkoxide clusters $[Yb_2K_{10}Na_6(OCH_2CH_2NMe_2)_{18}(OH)_4]$ (**4**) and $[Yb_2K_8Na_8(OCH_2CH_2NMe_2)_{18}(OH)_4]$ (**5**), respectively. These clusters were fully characterized by elemental analysis, IR, ^1H NMR, and single-crystal structural analysis. The heterometal alkoxide clusters **1**–**5** exhibited good catalytic activity for the ring-opening polymerization of ε-caprolactone (ε-CL). It is interesting to note that the catalytic activity of these heterometal alkoxide clusters increases with the increase of the molar ratio of alkali metal to lanthanide metal. For the same molar ratio of alkali metal to lanthanide metal, however, the catalytic activity of the heterometal clusters is highly dependent on the type and molar ratio of the alkali metal centers. The higher the molar ratio of potassium to sodium, the higher the catalytic activity.

Introduction

Two major motivations for researching heterometal clusters based on alkoxide ligands have been identified.[1–5] The first is that these heterometallic compounds are of interest due to their enhanced reactivity compared to their homometallic homologues arising from metal-metal interactions.[6–9] The second motivation is related to their application as materials. They can act as materials themselves or as precursors for more complicated materials such as superconductors.[10–13] Lanthanide–alkali metal alkoxide clusters are of particular interest for exploring lanthanide-doped materials, model systems, and efficient biheterometallic catalysts as well as for elucidating the mechanism of catalytic reactions.[14–19] However, a controllable method for rational synthesis is still a challenge as the chemistry of alkoxide clusters has been proven to be complicated − the reaction products depend on the stoichiometries of reagents as well as the central metal atoms.[1,20–21] To date, few methods for the rational synthesis of lanthanide–alkali metal alkoxide clusters have been reported. Recently, we have reported that adding a definite amount of NaOH into the reaction solution results in the rational preparation of lanthanide–sodium biheterometal alkoxide clusters containing a hydroxide group, $LnNa_8[OC(CH_3)_3]_{10}(OH)$[18] and $Ln_2Na_8(OCH_2CH_2NMe_2)_{12}(OH)_2$,[22] using self-assembly by hydroxide as a driving force. In addition, this approach has been proven to provide the products in high yields reproducibly. Importantly, these heterometal alkoxide clusters showed superior polymerization activity relative to previously reported homometallic catalysts. Thus inspired, we turned our attention toward designing novel lanthanide–alkali metal alkoxide clusters.

We have posed the question: what is the effect of changing the alkali metal and the molar ratio of alkali metal to lanthanide metal on the synthesis, crystal structure, and reactivity of the lanthanide–alkali metal alkoxide clusters? It is interesting to study the synthesis of the lanthanide–potassium biheterometal alkoxide clusters and the lanthanide–potassium–sodium triheterometal clusters by the same synthetic strategy of using hydroxide as a driving force through adding definite amounts of NaOH or KOH. With this in mind, we were prompted to further study the controllable synthesis of heterometal alkoxide clusters. Herein we report the synthesis and structural characterization of three lanthanide–potassium biheterometal alkoxide clusters, $[Ln_4K_{20}(OCH_2CH_2NMe_2)_{26}(OH)_6]$ [Ln = Nd (**1**), Pr (**2**), Yb (**3**)], and two lanthanide–potassium–sodium triheterometal alkoxide clusters, $[Yb_2K_{10}Na_6(OCH_2CH_2NMe_2)_{18}(OH)_4]$ (**4**) and $[Yb_2K_8Na_8(OCH_2CH_2NMe_2)_{18}(OH)_4]$ (**5**).

[a] School of Chemistry and Chemical Engineering & Key Laboratory of Environment-Friendly Polymer Materials of Anhui Province, Anhui University,
Hefei 230039, People's Republic of China
E-mail: sht_anda@126.com
[b] Key Laboratory of Organic Synthesis of Jiangsu Province, School of Chemistry and Chemical Engineering, Dushu Lake Campus, Suzhou University,
Suzhou 215123, People's Republic of China
E-mail: qshen@suda.edu.cn

Clusters **1**–**5** were tested for their catalytic activity in the ring-opening polymerization of ε-CL. Direct comparison of the reactivity of these clusters raises issues of importance for the design of new cyclic ester polymerization catalysts.

Results and Discussion

Synthesis and Characterization of Clusters 1–3

As reported previously, the addition of a definite amount of NaOH into the reaction solution results in the rational preparation of lanthanide–sodium biheteromeal alkoxide clusters containing a hydroxide group, $LnNa_8[OC(CH_3)_3]_{10}(OH)$[18] and $Ln_2Na_8(OCH_2CH_2NMe_2)_{12}(OH)_2$.[22] To understand the effect of the alkali metal on the synthesis, crystal structure, and reactivity of heterometal alkoxide clusters, the analogous reaction of $NdCl_3$ with 6.5 equiv. of $KOCH_2CH_2NMe_2$ and 1.5 equiv. of KOH was conducted in THF at room temperature, and afforded the much larger cluster $[Nd_4K_{20}(OCH_2CH_2NMe_2)_{26}(OH)_6]$ (**1**) in 62% yield (based on Nd); see Equation (1). The synthesis can be reproduced. To the best of our knowledge, this biheteromeal cluster is the largest one, which contains the maximum number of metal atoms.

$$4LnCl_3 + 26KOCH_2CH_2NMe_2 + 6KOH \longrightarrow Ln_4(OCH_2CH_2NMe_2)_{26}(OH)_6K_{20} + KCl \quad (1)$$

Ln = Nd (62%) Pr (53%) Yb (65%)

The metathesis reaction of $LnCl_3$ with alkali metal alkoxide was reported to be dependent on the central metal used. For example, the reaction of YCl_3 with $NaOCMe_3$ in a molar ratio of 1:3 afforded $Y_3(OCMe_3)_8Cl(THF)_2$, whereas the same reaction with $LaCl_3$ produced $La_3(OCMe_3)_9(THF)_2$.[20a] The synthesis of clusters of Pr and Yb was also attempted to evaluate the validity of this approach. The same reactions with $PrCl_3$ and $YbCl_3$, went smoothly and gave the corresponding clusters $[Pr_4K_{20}(OCH_2CH_2NMe_2)_{26}(OH)_6]$ (**2**) and $[Yb_4K_{20}(OCH_2CH_2NMe_2)_{26}(OH)_6]$ (**3**) in 53% and 65% yields, respectively. Clusters **1**–**3** are all soluble in THF and toluene but not in hexane. The results of elemental analysis of **1**–**3** were all identical to the calculated results. The ^1H NMR spectra for paramagnetic clusters **1**–**3** showed a very broad shift range.

Clusters **1**–**3** were further characterized by X-ray crystallography. The determination of crystal structures revealed that **1**–**3** have the same solid-state structure [Figure 1 (a)]. The crystal structure diagram with the $CH_2CH_2NMe_2$ groups omitted for clarity is shown in Figure 1 (b). Details of the crystallographic data are listed in Table 1, and selected bond lengths and angles are provided in Tables 2 and 3, respectively.

As shown in Figure 1, the clusters are centrosymmetric and the overall clusters in each case contain four lanthanide metal centers, 20 potassium metal atoms, 26

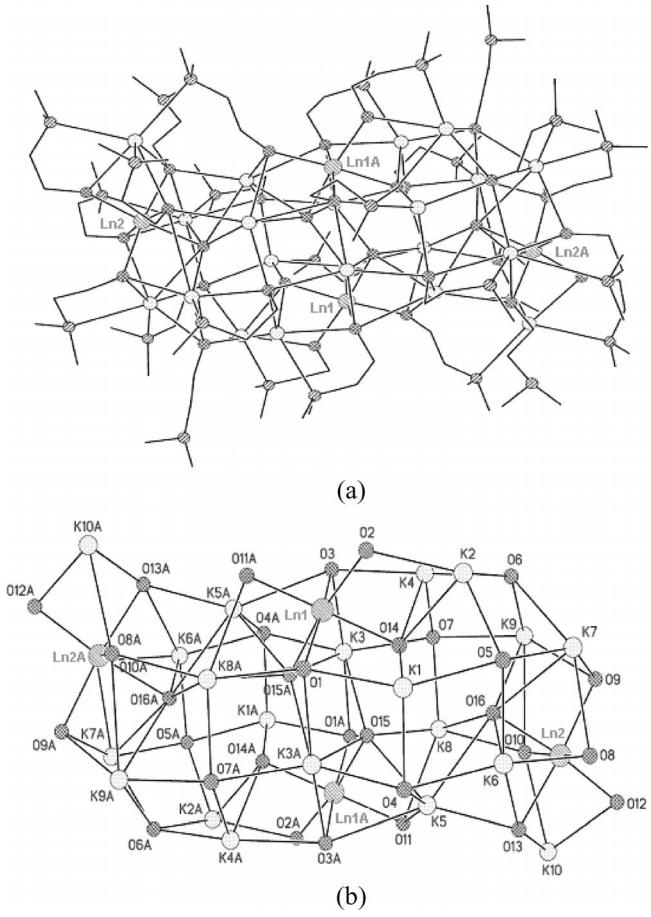

Figure 1. (a) Crystal structures of **1**–**3**; (b) Molecular structure of **1**–**3** with $CH_2CH_2NMe_2$ groups omitted for clarity (atomic displacement parameters set at 30%).

$OCH_2CH_2NMe_2$ groups, and six OH groups. Such persistence of the structure suggests that the framework is particularly stable. All the metal atoms are connected by μ-O bridges. Each lanthanide ion is coordinated to six oxygen atoms to form a distorted octahedron. There is a difference in the coordination environments between Ln(1), Ln(1A) and Ln(2), Ln(2A), in the former pair the six oxygen atoms come from four $OCH_2CH_2NMe_2$ groups and two OH groups and in the latter from five $OCH_2CH_2NMe_2$ groups and one OH group. The Ln–$OCH_2CH_2NMe_2$ bonds are of three types: Ln–μ_2-$OCH_2CH_2NMe_2$, Ln–μ_3-$OCH_2CH_2NMe_2$, and Ln–μ_4-$OCH_2CH_2NMe_2$. The average bond lengths of Ln–μ_2-$OCH_2CH_2NMe_2$ [2.284(4), 2.291(5), and 2.176(5) Å for **1**, **2**, and **3**, respectively], Ln–μ_3-$OCH_2CH_2NMe_2$ [2.318(4), 2.332(5), and 2.196(5) Å for **1**, **2**, and **3**, respectively], and Ln–μ_4-$OCH_2CH_2NMe_2$ [2.366(4), 2.376(5), and 2.242(5) Å for **1**, **2**, and **3**, respectively] are comparable when the differences in the ionic radii between Nd, Pr, and Yb are considered. The comparison of the data for **1** with other Nd clusters is given as an example. The average bond lengths of Nd–μ_2-$OCH_2CH_2NMe_2$ and Nd–μ_3-$OCH_2CH_2NMe_2$ are consistent with those of $Nd_2Na_8(OCH_2CH_2NMe_2)_{12}(OH)_2$, which has been reported previously.[22] The bond lengths are 2.286 and 2.368 Å for Nd–

Table 1. Details of the crystallographic data of **1**–**5**.

	1	**2**	**3**	**4**	**5**
Empirical formula	$C_{104}H_{266}N_{26}K_{20}O_{32}Nd_4\cdot(C_7H_8)$	$C_{111}H_{274}N_{26}K_{20}O_{32}Pr_4\cdot(C_7H_8)$	$C_{104}H_{266}N_{26}K_{20}O_{32}Yb_4\cdot(C_7H_8)$	$C_{72}H_{184}K_{10}N_{18}Na_6O_{22}Yb_2\cdot\mathbf{2}(C_7H_8)$	$C_{72}H_{184}K_8N_{18}Na_8O_{22}Yb_2\cdot0.5(C_6H_{14})$
Fw	3832.51	3831.20	3959.72	2713.66	2540.26
T [K]	153(2)	153(2)	153(2)	153(2)	193(2)
Wavelength [Å]	0.71070	0.71070	0.71070	0.71070	0.71070
Crystal system	monoclinic	monoclinic	monoclinic	monoclinic	triclinic
Space group	$P2_1/n$	$P2_1/n$	$P2_1/n$	$P2_1/n$	$P\bar{1}$
a [Å]	22.8863(13)	22.939(3)	22.7352(19)	15.4461(14)	14.2214(13)
b [Å]	15.9806(8)	15.9722(16)	15.9230(13)	19.2367(17)	18.5570(19)
c [Å]	26.0245(15)	26.013(3)	25.907(2)	22.348(2)	24.788(2)
α [°]	90	90	90	90	101.543(2)
β [°]	105.0950(10)	105.111(3)	105.278(2)	91.159(2)	92.707(3)
γ [°]	90	90	90	90	100.098(3)
V [Å]^3	9189.7(9)	9201.4(18)	9047.1(13)	6639.1(10)	6287.1(11)
Z	2	2	2	2	2
D_{calc} [mg m^{-3}]	1.385	1.383	1.454	1.357	1.342
Abs. coeff. [mm]$^{-1}$	1.628	1.556	2.573	1.795	1.832
F(000)	3984	3988	4076	2828	2646
Theta range [°]	3.02–25.35	3.02–25.35	3.03–25.35	3.00–25.35	3.02–25.35
Collected refl.	88301	89127	86823	64602	62249
Independent refl.	16775 [R(int) = 0.0465]	16825 [R(int) = 0.0699]	16555 [R(int) = 0.0573]	12122 [R(int) = 0.0557]	22831 [R(int) = 0.0731]
R [$I>2\sigma(I)$]	0.0533	0.0755	0.0589	0.0522	0.0760
Rw	0.1239	0.1504	0.1263	0.1110	0.1921
Goodness-of-fit on F^2	1.117	1.149	1.112	1.136	1.068

μ_2-$OCH_2CH_2NMe_2$ and Nd–μ_3-$OCH_2CH_2NMe_2$, respectively. Moreover, the bond length sequence of Ln–μ_2-$OCH_2CH_2NMe_2$ < Ln–μ_3-$OCH_2CH_2NMe_2$ < Ln–μ_4-$OCH_2CH_2NMe_2$ observed here is reasonable and is seen in other alkoxide clusters.[23–24]

Table 2. Selected bond lengths [Å] for **1**–**3**.

	1	**2**	**3**
Ln(1)–O(11)A	2.283(3)	2.301(5)	2.175(4)
Ln(1)–O(2)	2.317(4)	2.327(5)	2.199(5)
Ln(1)–O(14)	2.344(4)	2.349(5)	2.222(4)
Ln(1)–O(15)A	2.348(3)	2.353(5)	2.225(5)
Ln(1)–O(3)	2.377(3)	2.394(5)	2.245(5)
Ln(1)–O(1)	2.386(3)	2.402(5)	2.258(5)
Ln(2)–O(12)	2.251(4)	2.255(5)	2.153(5)
Ln(2)–O(8)	2.326(4)	2.340(5)	2.203(5)
Ln(2)–O(9)	2.346(4)	2.356(5)	2.209(5)
Ln(2)–O(16)	2.366(4)	2.372(5)	2.244(5)
Ln(2)–O(13)	2.369(4)	2.387(5)	2.251(5)
Ln(2)–O(10)	2.373(4)	2.375(5)	2.258(5)

Table 3. Selected angles [°] for **1**–**3**.

	1	**2**	**3**
O(11)A–Ln(1)–O(14)	175.70(12)	175.64(17)	177.72(17)
O(2)–Ln(1)–O(3)	99.68(15)	100.2(2)	96.7(2)
O(15)A–Ln(1)–O(3)	84.69(12)	84.36(17)	86.11(18)
O(2)–Ln(1)–O(1)	93.02(15)	93.0(2)	93.08(19)
O(15)A–Ln(1)–O(1)	82.62(12)	82.50(16)	84.26(17)
O(12)–Ln(2)–O(9)	98.98(14)	99.05(19)	97.2(2)
O(13)–Ln(2)–O(16)	85.13(13)	85.13(18)	84.59(19)
O(9)–Ln(2)–O(16)	87.48(13)	87.27(18)	90.04(19)
O(8)–Ln(2)–O(10)	172.57(13)	172.42(17)	174.65(17)
O(12)–Ln(2)–O(13)	88.60(15)	88.73(19)	88.3(2)

The coordination environments around the K atoms can be divided into four classes. K(1), K(1)A, K(2), K(2)A, K(4), and K(4)A are five-coordinate distorted trigonal bipyramids with four oxygen atoms and one nitrogen atom; K(3), K(3)A, K(5), K(5)A, K(8), and K(8)A are six-coordinate distorted octahedra with six oxygen atoms; K(6), K(6)A, K(7), K(7)A, K(9), and K(9)A are six-coordinate distorted octahedra with five oxygen atoms and one nitrogen atom, and K(10) and K(10)A are six-coordinate distorted octahedra with three oxygen atoms and three nitrogen atoms. The average bond lengths of K–$OCH_2CH_2NMe_2$ for **1**, **2**, and **3** are normal and comparable to each other.

Synthesis and Characterization of Clusters 4 and 5

The next question to be addressed after we had obtained the lanthanide–sodium and lanthanide–potassium alkoxide clusters was whether we could synthesize the lanthanide–potassium–sodium alkoxide clusters by the same strategy. We attempted the reaction of $YbCl_3$, $KOCH_2CH_2N(CH_3)_2$, and NaOH in a molar ratio of 1:9:3 in THF at room temperature and obtained the lanthanide–potassium–sodium triheterometal alkoxide cluster $[Yb_2K_{10}Na_6(OCH_2CH_2NMe_2)_{18}(OH)_4]$ (**4**). To evaluate the validity of the test, the same reaction with $YbCl_3$, $KOCH_2CH_2N(CH_3)_2$, and NaOH in a different molar ratio of 1:9:4 went smoothly and gave another lanthanide–potassium–sodium triheterometal alkoxide cluster $[Yb_2K_8Na_8(OCH_2CH_2NMe_2)_{18}(OH)_4]$ (**5**); see Equation (2). These results validate that this strategy of self-assembly with hydroxide as a driving force is credible.

$$4LnCl_3 + 26KOCH_2CH_2NMe_2 + 6KOH \longrightarrow Ln_4(OCH_2CH_2NMe_2)_{26}(OH)_6K_{20} + KCl$$

Ln = Nd (62%) Pr (53%) Yb (65%)

$$2YbCl_3 + 18KOCH_2CH_2NMe_2 + 6NaOH \longrightarrow Yb_2(OCH_2CH_2NMe_2)_{18}(OH)_4K_{10}Na_6 + 6KCl + 2KOH \quad (2)$$

yield 48%

$$2YbCl_3 + 18KOCH_2CH_2NMe_2 + 8NaOH \longrightarrow Yb_2(OCH_2CH_2NMe_2)_{18}(OH)_4K_8Na_8 + 6KCl + 4KOH$$

yield 39%

Clusters **4** and **5** are both soluble in THF and toluene but not in hexane. The results of elemental analysis for **4** and **5** were identical to the calculated results, and inductively coupled plasma (ICP) analysis indicated that the molar ratios of potassium metal to sodium metal were 5:3 and 1:1 for **4** and **5**, respectively. The ^{1}H NMR spectra of **4** and **5** showed a very broad shift range arising from paramagnetism. Clusters **4** and **5** were further characterized by X-ray crystallography. The crystal structure diagrams with $CH_2CH_2NMe_2$ groups omitted for clarity are shown in Figures 2 and 3. Details of the crystallographic data are listed in Table 1, and selected bond lengths and bond angles are provided in Tables 4 and 5, respectively.

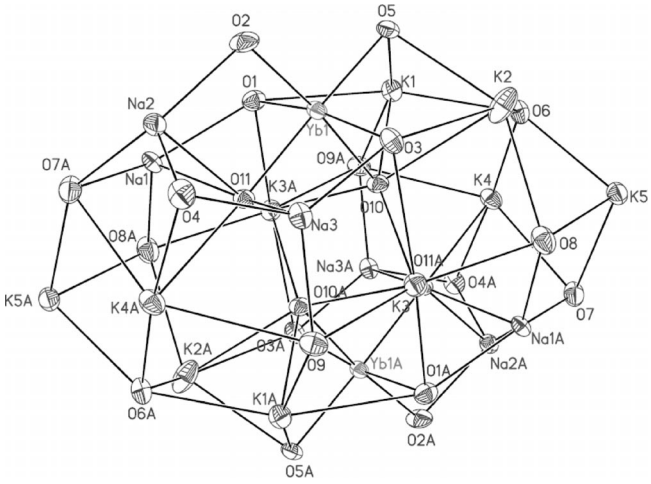

Figure 2. Molecular structure of **4** with $CH_2CH_2NMe_2$ groups omitted for clarity (atomic displacement parameters set at 30%).

As shown in Figure 2, **4** is centrosymmetric and the overall structure contains two ytterbium metal centers, ten potassium metal atoms, six sodium metal atoms, 18 $OCH_2CH_2NMe_2$ groups, and four OH groups. All the metal centers are connected by μ-O bridge bonds. Each ytterbium atom is coordinated by four oxygen atoms [O(1), O(2), O(3), O(5)] from $OCH_2CH_2NMe_2$ groups and two [O(10), O(11)] from OH groups. The coordination geometry around the lanthanide atom is best described as distorted

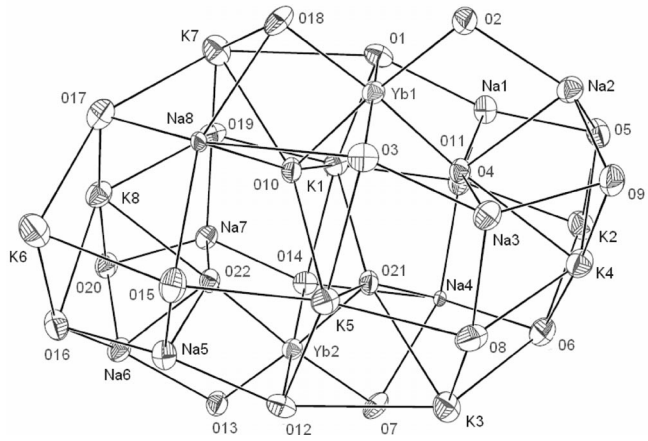

Figure 3. Molecular structure of **5** with $CH_2CH_2NMe_2$ groups omitted for clarity (atomic displacement parameters set at 30%).

Table 4. Selected bond lengths [Å] and angles [°] for **4**.

Atoms	Distance	Atoms	Distance
Yb(1)–O(2)	2.159(4)	Yb(1)–O(5)	2.194(4)
Yb(1)–O(3)	2.239(4)	Yb(1)–O(1)	2.240(4)
Yb(1)–O(11)	2.242(3)	Yb(1)–O(10)	2.246(4)
Atoms	**Angle**	**Atoms**	**Angle**
O(2)–Yb(1)–O(3)	95.41(16)	O(2)–Yb(1)–O(1)	93.28(16)
O(5)–Yb(1)–O(11)	177.77(13)	O(3)–Yb(1)–O(10)	85.89(14)
O(1)–Yb(1)–O(10)	84.94(14)		

Table 5. Selected bond lengths [Å] and angles [°] for **5**.

Atoms	Distance	Atoms	Distance
Yb(1)–O(2)	2.152(6)	Yb(1)–O(7)	2.208(6)
Yb(1)–O(11)	2.247(6)	Yb(1)–O(3)	2.249(5)
Yb(1)–O(1)	2.256(6)	Yb(1)–O(10)	2.259(6)
Yb(2)–O(13)	2.160(6)	Yb(2)–O(18)	2.185(6)
Yb(2)–O(12)	2.240(6)	Yb(2)–O(21)	2.247(6)
Yb(2)–O(22)	2.248(6)	Yb(2)–O(14)	2.264(6)
Atoms	**Angle**	**Atoms**	**Angle**
O(7)–Yb(1)–O(1)	95.4(2)	O(2)–Yb(1)–O(10)	174.7(2)
O(1)–Yb(1)–O(11)	87.2(2)	O(7)–Yb(1)–O(3)	89.6(2)
O(11)–Yb(1)–O(3)	87.1(2)		
O(18)–Yb(2)–O(12)	96.4(2)	O(13)–Yb(2)–O(21)	176.2(2)
O(12)–Yb(2)–O(22)	87.4(2)	O(18)–Yb(2)–O(14)	88.9(2)
O(22)–Yb(2)–O(14)	86.5(2)		

octahedral geometry, in which O(1), O(2), O(3), and O(10) can be considered to occupy equatorial positions with the sum of angles around the lanthanide center of ΣO–Ln–O being 359.5°. O(11) and O(5) occupy axial positions with the O(5)–Ln–O(11) angle of 177.8°, which is slightly distorted from the idealized value of 180°.

The Ln–$OCH_2CH_2NMe_2$ bonds are of three types: Ln–μ_2-$OCH_2CH_2NMe_2$, Ln–μ_3-$OCH_2CH_2NMe_2$, and Ln–μ_4-$OCH_2CH_2NMe_2$. The average bond lengths of Ln–$OCH_2CH_2NMe_2$ are 2.159(4) Å for Ln–μ_2-$OCH_2CH_2NMe_2$, 2.194(3) Å for Ln–μ_3-$OCH_2CH_2NMe_2$, and 2.242(4) Å for Ln–μ_4-$OCH_2CH_2NMe_2$. The 0.08 Å increase for Ln–μ_2-$OCH_2CH_2NMe_2$ and 0.05 Å increase for Ln–μ_3-OCH_2-

CH_2NMe_2 in comparison with Ln–μ_4-$OCH_2CH_2NMe_2$ is reasonable and has been observed in other alkoxide complexes.[25]

As shown in Figure 3, **5** is composed of two ytterbium metal atoms, eight potassium metal atoms, eight sodium metal atoms, 18 $OCH_2CH_2NMe_2$ groups, and four OH groups. All the metal centers are connected by μ-O bridge bonds. Each ytterbium atom is coordinated to four oxygen atoms from $OCH_2CH_2NMe_2$ groups [{O(1), O(2), O(3), O(7)} for Yb1 and {O(12), O(13), O(14), O(18)} for Yb2] and two oxygen atoms from OH groups [{O(10), O(11)} for Yb1 and {O(21), O(22)} for Yb2] to form distorted octahedra.

The Ln–$OCH_2CH_2NMe_2$ bonds are of three types: Ln–μ_2-$OCH_2CH_2NMe_2$, Ln–μ_3-$OCH_2CH_2NMe_2$, and Ln–μ_4-$OCH_2CH_2NMe_2$. The average bond lengths of Ln–$OCH_2CH_2NMe_2$ are 2.173(4) Å for Ln–μ_2-$OCH_2CH_2NMe_2$, 2.185(3) Å for Ln–μ_3-$OCH_2CH_2NMe_2$, and 2.251(4) Å for Ln–μ_4-$OCH_2CH_2NMe_2$. The 0.08 Å increase for Ln–μ_2-$OCH_2CH_2NMe_2$ and 0.06 Å increase for Ln–μ_3-$OCH_2CH_2NMe_2$ in comparison with Ln–μ_4-$OCH_2CH_2NMe_2$ are reasonable, and we found that **4** and **5** are homologous in the bond length of Ln–$OCH_2CH_2NMe_2$.

However, there is a difference in the coordination environments around the alkali metal centers between **4** and **5**. The coordination environment around the K ions of **4** can be divided into four classes. K(1), K(1)A, K(4), and K(4)A are six-coordinate distorted octahedra with five oxygen atoms and one nitrogen atom, K(2) and K(2)A are seven-coordinate with five oxygen atoms and two nitrogen atoms, K(5) and K(5)A are six-coordinate with three oxygen atoms and three nitrogen atoms, and K(3) and K(3)A are six-coordinate with six oxygen atoms. All of the Na atoms in **4** are five-coordinate distorted trigonal bipyramids with four oxygen atoms and one nitrogen atom. The coordination environment around the K ions of **5** can also be divided into four classes. The K(1) and K(5) are six-coordinate with six oxygen atoms, K(2) and K(6) are six-coordinate with three oxygen atoms and three nitrogen atoms, K(3) and K(7) are seven-coordinate with five oxygen atoms and two nitrogen atoms, and K(4) and K(8) are six-coordinate with five oxygen atoms and one nitrogen atom. The coordination environment around the Na ions of **5** can be divided into two classes. Na(1), Na(2), Na(3), Na(5), Na(6), and Na(7) are five-coordinate with four oxygen atoms and one nitrogen atom, whereas Na(4) and Na(8) are four-coordinate with four oxygen atoms.

Catalytic Activity of Clusters 1–5 for Ring-Opening Polymerization of ε-Caprolactone (ε-CL)

The ring-open polymerization of lactones has attracted much interest because of their biological and mechanical properties. Recently, we have reported that lanthanide–sodium biheterometal alkoxide clusters show much higher reactivity than the related neutral complexes without alkali metal ions for the ring opening polymerization of ε-CL.[18,22] It is important to understand whether the lanthanide–potassium biheterometal clusters and lanthanide–potassium–sodium triheterometal clusters can be used as single component catalysts and to study their catalytic behavior in detail. We have tested the reactivity of **1**–**5** for the ring-opening polymerization of ε-CL. The preliminary results are shown in Table 6. The data previously reported for some other complexes, such as $Nd(OCH_2CH_2NMe_2)_3$, $KOCH_2CH_2NMe_2$, and $Yb_2Na_8(OCH_2CH_2NMe_2)_{12}(OH)_2$ (**6**), are also included for comparison.

Table 6. Polymerization of ε-CL initiated by **1**–**6**.[a]

Entry	Init	[M]/[I]	Time [min]	Conv.[b] [%]	M_n ($\times 10^4$)	M_w/M_n[c]
1	**1**	10000	1	100	5.23	1.78
2	**1**	15000	1	100	5.58	1.69
3	**1**	20000	1	100	5.89	1.75
4	**2**	10000	1	100	4.04	1.38
5	**2**	15000	1	86	5.72	1.46
6	**3**	10000	1	76	4.57	1.66
8	**4**	10000	1	100	8.28	1.84
9	**4**	15000	1	100	7.93	1.80
10	**5**	10000	1	100	8.37	1.82
11	**5**	15000	1	67	8.60	1.64
12	KOR[d]	200	60	0	0	
13	$Nd(OR)_3$[d]	1500	60	0	0	
14	**6**[e]	6000	1	75	3.9	1.56

[a] Conditions: [cat] = 0.01 mol/L, toluene as solvent, $Vs_{ol.}/V_{mon.}$ = 5:1. [b] Conv.: weight of polymer obtained/weight of monomer used. [c] Measured by GPC calibrated with standard polystyrene samples. [d] OR = $OCH_2CH_2NMe_2$. [e] **6** = $Yb_2Na_8(OCH_2CH_2NMe_2)_{12}(OH)_2$.

It can be seen that clusters **1**–**5** show extremely high activity. Taking cluster **1** as an example, it can be seen that the polymerization proceeded rapidly and was completed in less than 1 min at ambient temperature when the molar ratio of [CL] to [I] (where I indicates **1**) is 15000:1. When the molar ratio of [CL] to [I] increases to 20000:1, the polymerization still gives a yield as high as 100% under the same conditions (Table 6, entries 1–3). The activity of **1** reaches as high as 1.2×10^5 kg/mol h. To the best of our knowledge, this is the highest activity for the polymerization of ε-CL.[22,26] This is in striking contrast to the reactions with $K(OCH_2CH_2NMe_2)$ or $Nd(OCH_2CH_2NMe_2)_3$. In both cases no reaction was observed under the same conditions (Table 6, entries 12 and 13), although $Y(OCH_2CH_2NMe_2)_3$ has been reported to be efficient initiator for the polymerization.[27] For clusters **1**–**3**, we found the reactivity depended profoundly on the lanthanide metal present. For example, when the molar ratio of [CL] to [I] was 10000, the conversion was as high as 100% for **2** but only 76% for **3** (Table 6, entries 1, 4, and 6). The activity sequence of Yb < Pr ≈ Nd observed here is consistent with the increase in the ionic radius, which is similar to those found in polymerization systems with neutral lanthanide phenoxide and lanthanocene-based catalysts.[28,29]

To further understand the effect of the alkali metal on the catalytic activity, we compared the activity of $[Yb_4K_{20}(OCH_2CH_2NMe_2)_{26}(OH)_6]$ (**3**), $[Yb_2K_{10}Na_6(OCH_2$-

$CH_2NMe_2)_{18}(OH)_4]$ (**4**), $[Yb_2K_8Na_8(OCH_2CH_2NMe_2)_{18}(OH)_4]$ (**5**), and $Yb_2Na_8(OCH_2CH_2NMe_2)_{12}(OH)_2$ (**6**), which all contain the same central metal, Yb. These clusters all showed an unexpectedly high activity. Such high activities for these heterometal clusters may be attributed to the cooperation of lanthanide and alkali metal centers, which results from the concomitant coordination of the monomer to both metal atoms.[22,30] Therefore, the catalytic activity of these clusters increases with the increase of the molar ratio of alkali metal to lanthanide metal. For example, the activity sequence of **6** < **3** < **5** is consistent with the increase of the molar ratio of the alkali metal to the lanthanide metal (**6** [4:1] < **3** [5:1] < **5** [8:1]) (Table 6, entries 6, 8, and 14). For the same molar ratio of the alkali metal to lanthanide metal, we found that the catalytic activity is still dependent on the molar ratio of potassium to sodium. The activity sequence of **5** < **4** is attributed to the molar ratio of potassium to sodium, 1:1 for **5** and less than 5:3 for **4**, as the molar ratio of alkali metal to lanthanide metal in both **4** and **5** is 8:1 (Table 6, entries 9 and 11). Cluster **4** has the best catalytic activity due to the higher coordination activity of potassium to the ε-CL monomer than sodium.[31] The catalytic activity was enhanced with the increase of the molar ratio of potassium to sodium, where the ratio of alkali metal to lanthanide metal is same. In addition, all the gel permeation chromatography (GPC) curves of the polymers obtained with clusters **1**–**5** were unimodal with relatively narrow molecular weight distributions (M_w/M_n in the range of 1.38–1.84, Table 6). The molecular weights of the resulting polymers were lower than those expected from the monomer-to-cluster ratio, suggesting that transfer reactions may take place in the system. These results clearly indicate that the heterometal clusters **1**–**5** could be used as single-component catalysts.

Conclusions

In summary, we have successfully synthesized and structurally characterized a series of biheterometal clusters $[Ln_4K_{20}(OCH_2CH_2NMe_2)_{26}(OH)_6]$ [Ln = Nd (**1**), Pr (**2**), Yb (**3**)] and triheterometal clusters $[Yb_2K_{10}Na_6(OCH_2CH_2NMe_2)_{18}(OH)_4]$ (**4**) and $[Yb_2K_8Na_8(OCH_2CH_2NMe_2)_{18}(OH)_4]$ (**5**) in high yields. These heterometal alkoxide clusters **1**–**5** were found to be efficient catalysts for the ring-opening polymerization of ε-CL as single-component catalysts. All the polymers obtained showed unimodal GPC curves with relatively narrow molecular weight distributions. The catalytic activity of these clusters increases with the increase of the molar ratio of alkali metal to lanthanide metal. For the same molar ratio, we found the catalytic activity of these clusters is dependent on the type and molar ratio of the alkali metal centers. The higher the molar ratio of potassium metal to sodium metal, the higher the catalytic activity. A further study on the synthesis of the lanthanide–alkali metal alkoxide clusters and their catalytic activity in the homogeneous catalysis is ongoing in our laboratory.

Experimental Section

General Procedures: All manipulations were performed under argon, using standard Schlenk techniques. THF and toluene were distilled from sodium benzophenone ketyl before use. ε-CL was purchased from Acros, dried with CaH_2 for 48 h, and distilled under reduced pressure. Lanthanide metal analyses were carried out by EDTA titration with an xylenol orange indicator and a hexamine buffer. Carbon and hydrogen analyses were performed by direct combustion with a Carlo–Erba EA-1110 instrument. Alkali metal analyses were performed with IRIS Intrepid II ICP-OES equipment. IR spectra were recorded with a Nicolet-550 FT-IR spectrometer from KBr pellets. Melting points of the clusters were measured in sealed capillaries and are uncorrected. ^1H NMR spectra were measured with a Unity Inova-400 spectrometer in deutered benzene (C_6D_6) at 25°C. Molecular weights and molecular weight distributions were determined against polystyrene standards by GPC at 40 °C with a Water 1515 apparatus with three HR columns (HR-1, HR-2, and HR-4) and an ultraviolet visible detector using THF as the eluent.

Synthesis of $[Nd_4K_{20}(OCH_2CH_2NMe_2)_{26}(OH)_6]$ (1): A Schlenk flask was charged with K (0.62 g, 16 mmol), THF (35 mL), and a stirrer bar. To this solution was added $HOCH_2CH_2NMe_2$ (1.3 mL, 13 mmol) and the reaction immediately gave H_2 and $KOCH_2CH_2NMe_2$. After 24 h, a pale-gray slurry of $NdCl_3$ (0.50 g, 2 mmol) in THF (15 mL) was added. The solution was stirred for 2 h at room temperature before KOH (0.17 g, 3 mmol) was added. The resulting solution was stirred for another 48 h before the solvents were removed under vacuum. The residue was extracted into toluene and KCl was removed by centrifugation. After the extractants were concentrated, light blue crystals of **1** were obtained at room temperature after several days; yield 1.19 g (62% based on Nd); m.p. 228–231 °C (dec.). $C_{104}H_{266}K_{20}N_{26}Nd_4O_{32}$ (3832.51 g mol^{-1}): calcd. C 33.29, H 7.15, N 9.71, Nd 15.38; found C 33.26, H 7.45, N 9.36, Nd 15.30. IR (KBr pellet): $\tilde{\nu}$ = 3420 (s), 2952 (m), 2865 (w), 2829 (m), 2784 (m), 2538 (w), 1655 (s), 1458 (s), 1396 (s), 1300 (m), 1238 (m), 1158 (m), 1087 (w), 1038 (m), 947 (w), 876 (w), 776 (m), 638 (w), 504 (m).

Synthesis of $[Pr_4K_{20}(OCH_2CH_2NMe_2)_{26}(OH)_6]$ (2): Using the same procedure as described above for **1**, colorless crystals of **2** were prepared from $PrCl_3$ (0.49 g, 2 mmol), $KOCH_2CH_2NMe_2$, and KOH; yield 1.02 g (53% based on Pr); m.p. 227–232 °C (dec.). $C_{104}H_{266}K_{20}N_{26}O_{32}Pr_4$ (3831.20 g mol^{-1}): calcd. C 33.41, H 7.17, N 9.74, Pr 15.07; found C 33.24, H 7.31, N 9.66, Pr 15.00. IR (KBr pellet): $\tilde{\nu}$ = 3380 (s), 1636 (m), 1389 (s), 1245 (s), 1158 (s), 1058 (w), 880 (m), 633 (m), 556 (m), 502 (s) cm^{-1}.

Synthesis of $[Yb_4K_{20}(OCH_2CH_2NMe_2)_{26}(OH)_6]$ (3): Using the same procedure as described above for **1**, colorless crystals of **3** were prepared from $YbCl_3$ (0.56 g, 2 mmol), $KOCH_2CH_2NMe_2$, and KOH; yield 1.29 g (65% based on Yb); m.p. 220–224 °C (dec.). $C_{104}H_{266}K_{20}N_{26}O_{32}Yb_4$ (3959.72 g mol^{-1}): calcd. C 32.30, H 6.93, N 9.42, Yb 17.90; found C 32.43, H 6.94, N 9.44, Yb 17.88. IR (KBr pellet): $\tilde{\nu}$ = 3433 (s), 2954 (m), 2865 (w), 2829 (m), 2784 (m), 1655 (s), 1458 (m), 1397 (s), 1301 (s), 1240 (s), 1157 (s), 1093 (m), 1038 (m), 948 (w), 876 (w), 778 (w), 639 (m), 555 (w), 504 (m).

Synthesis of $[Yb_2K_{10}Na_6(OCH_2CH_2NMe_2)_{18}(OH)_4]$ (4): A Schlenk flask was charged with K (0.82 g, 21 mmol), THF (40 mL), and a stirrer bar. To this solution was added $HOCH_2CH_2NMe_2$ (1.8 mL, 18 mmol), and the reaction immediately gave H_2 and $KOCH_2CH_2NMe_2$. After 24 h, a pale-gray slurry of $YbCl_3$ (0.56 g, 2 mmol) in THF (15 mL) was added. The solution was stirred for 2 h at room temperature before NaOH (0.24 g, 6 mmol) was added.

The resulting solution was stirred for a further 48 h and the solvents were removed under vacuum. The residue was extracted into toluene and NaCl and KCl were removed by centrifugation. After the extractants were concentrated, colorless crystals of **4** were obtained at room temperature after several days; yield 1.30 g (48% based on Yb); m.p. 199–202 °C (dec.). $C_{86}H_{200}K_{10}N_{18}Na_6O_{22}Yb_2$ (2713.66 g mol^{-1}): calcd. C 38.06, H 7.43, N 9.29, Yb 12.25; found C 37.24, H 7.35, N 9.07, Yb 12.17. IR (KBr pellet): $\tilde{\nu}$ = 3326 (s), 1598 (m), 1551 (m), 1389 (s), 1243 (m), 1165 (m), 1088 (w), 1042 (s), 880 (m), 671 (s), 509 (m).

Synthesis of $[Yb_2K_8Na_8(OCH_2CH_2NMe_2)_{18}(OH)_4]$ (5): Using the same procedure as described above for **4**, colorless crystals of **5** were prepared from $YbCl_3$ (0.56 g, 2 mmol), $KOCH_2CH_2NMe_2$ (18 mmol), and NaOH (0.32 g, 8 mmol); yield 0.99 g (39% based on Yb); m.p. 204–206 °C (dec.). $C_{75}H_{191}K_8N_{18}Na_8O_{22}Yb_2$ (2540.26 g mol^{-1}): calcd. C 35.46, H 7.58, N 9.93, Yb 13.62; found C 34.77, H 7.52, N 9.47, Yb 13.57. IR (KBr pellet): $\tilde{\nu}$ = 3307 (s), 1598 (s), 1532 (m), 1408 (s), 1337 (s), 1165 (w), 1082 (m), 1042 (w), 873 (m), 778 (m), 682 (s), 510 (m) cm^{-1}.

X-ray Structural Determination: Suitable single crystals of **1**, **2**, **3**, **4**, and **5** were sealed in thin-walled glass capillaries. Intensity data were collected with a Rigaku Mercury CCD area detector in ω scan mode using Mo-K_α radiation (λ = 0.71070 Å). The diffracted intensities were corrected for Lorentz polarization effects and empirical absorption corrections. Details of the intensity data collection and crystal data are given in Table 1. The structures were solved by direct methods and refined by full-matrix least-squares procedures based on $|F|^2$. All non-hydrogen atoms were refined anisotropically. The hydrogen atoms were all generated geometrically (C–H bond lengths fixed at 0.95 Å), assigned appropriate isotropic thermal parameters, and allowed to ride on their parent carbon atoms. All hydrogen atoms were held stationary and included in the structure factor calculation in the final stage of full-matrix least-squares refinement. The structures were solved and refined by using the SHELXL-97 program.[32]

CCDC-784297 (for **1**), -784298 (for **2**), -784299 (for **3**), -784300 (for **4**), and -784301 (for **5**) contain the supplementary crystallographic data for this paper. These data can be obtained free of charge from the Cambridge Crystallographic Data Centre via www.ccdc.cam.ac.uk/data_request/cif.

Typical Polymerization Procedure: All polymerizations were carried out in a 50 mL Schlenk flask under a dry Ar atmosphere. A typical polymerization reaction is given below. A 50 mL Schlenk flask equipped with a magnetic stirrer bar was charged with a solution of ε-CL (1 mL) in toluene (9.91 mL). To this solution was added a solution of **1** (0.09 mL) in toluene (1.0×10^{-2} M) using a rubber septum and syringe. The contents of the flask were vigorously stirred for 1 min at 25 °C. The polymerization was quenched by the addition of ethanol with 5% HCl. The precipitated product was washed with ethanol three times and dried in vacuo at room temperature overnight. The polymer yield was determined gravimetrically.

Acknowledgments

We are indebted to the Chinese National Natural Science Foundation (grant number 20902001), the Anhui Provincial Natural Science Foundation (grant number 090416220), and the 211 Project of Anhui University (grant number 2009QN014A) for financial support.

[1] A. Singh, R. C. Mehrotra, *Coord. Chem. Rev.* **2004**, *248*, 101–118.
[2] a) G. B. Nikiforov, H. W. Roesky, P. G. Jones, *Dalton Trans.* **2007**, *37*, 4149–4159; b) S. K. Mandal, P. M. Gurubasavaraj, H. W. Roesky, *Inorg. Chem.* **2007**, *46*, 7594–7600; c) E. V. Dikarev, H. T. Zhang, B. Li, *Angew. Chem. Int. Ed.* **2006**, *45*, 5448–5451; d) W. Maudez, M. Meuwly, K. M. Fromm, *Chem. Eur. J.* **2007**, *13*, 8302–8316.
[3] a) M. Mehring, D. Mansfeld, B. Costisella, M. Schurmann, *Eur. J. Inorg. Chem.* **2006**, *4*, 735–739; b) M. Mehring, D. Mansfeld, S. Paalasmaa, M. Schurmann, *Chem. Eur. J.* **2006**, *12*, 1767–1781.
[4] a) Z. Yang, X. Ma, H. W. Roesky, *Inorg. Chem.* **2007**, *46*, 7093–7096; b) P. C. Andrikopoulos, D. R. Armstrong, E. Hevia, *Organometallics* **2006**, *25*, 2415–2418; c) E. Hevia, K. W. Henderson, A. R. Kennedy, *Organometallics* **2006**, *25*, 1778–1785.
[5] a) D. V. Drobot, G. A. Seisenbaeva, V. G. Kessler, P. A. Scheglov, O. A. Nikonova, S. N. Michnevich, O. V. Petrakova, *J. Cluster Sci.* **2009**, *20*, 23–36; b) X. D. Kou, X. Y. Wang, D. Mendoza-Espinosa, L. N. Zakharov, A. L. Rheingold, W. H. Watson, K. A. Brien, L. K. Jayarathna, T. A. Hanna, *Inorg. Chem.* **2009**, *48*, 11002–11016.
[6] a) V. G. Kessler, S. Gohil, M. Kritikos, *Polyhedron* **2001**, *20*, 915–922; b) Y. K. Gun ko, U. Cristmann, V. G. Kessler, *Eur. J. Inorg. Chem.* **2002**, 1029; c) D. S. McGuiness, E. L. Marshall, V. C. Gibson, J. W. Steed, *J. Polym. Sci., Part A: Polym. Chem.* **2003**, *41*, 3798.
[7] J. F. Chai, V. Jancik, S. Singh, *J. Am. Chem. Soc.* **2005**, *127*, 7521–7528.
[8] a) R. E. Mulvey, *Organometallics* **2006**, *25*, 1060–1075; b) P. M. Gurubasavaraj, H. W. Roesky, P. M. V. Sharma, *Organometallics* **2007**, *26*, 3346–3351.
[9] a) Y. K. Gun'ko, U. Cristmann, V. G. Kessler, *Eur. J. Inorg. Chem.* **2002**, 1029; b) D. S. McGuiness, E. L. Marshall, V. C. Gibson, J. W. Steed, *J. Polym. Sci., Part A: Polym. Chem.* **2003**, *41*, 3798.
[10] a) E. Colacio, J. P. Costes, J. M. Dominguez-Vera, *Chem. Commun.* **2005**, 534–536; b) A. Mishra, W. Wernsdorfer, K. A. Abboud, *J. Am. Chem. Soc.* **2004**, *126*, 15648–15649.
[11] H. C. Aspinall, J. F. Bickley, J. M. Gaskell, A. C. Jones, G. Labat, P. R. Chalker, P. A. Williams, *Inorg. Chem.* **2007**, *46*, 5852–5860.
[12] M. Mehring, *Coord. Chem. Rev.* **2007**, *251*, 974–1006.
[13] J. K. Xiang, P. R. Yan, S. L. La, P. Z. Zhi, N. Gary, B. H. Rong, S. Z. Lan, *Inorg. Chem.* **2008**, *47*, 2728–2739.
[14] a) S. Habaue, M. Yoshikawa, Y. Okamoto, *Polym. J.* **1995**, *27*, 986; b) J. Chai, V. Jancik, S. Singh, H. Zhu, C. He, H. W. Roesky, H. G. Schmidt, M. Noltemeyer, N. S. Hosmane, *J. Am. Chem. Soc.* **2005**, *127*, 7521.
[15] a) F. G. Yuan, H. Y. Wang, Y. Zhang, *Chin. J. Chem.* **2005**, *23*, 409–412; b) H. M. Peng, Y. M. Yao, M. Y. Deng, Y. Zhang, Q. Shen, *J. Rare Earths* **2006**, *24*, 509.
[16] a) W. Maudez, M. Meuwly, K. M. Fromm, *Chem. Eur. J.* **2007**, *13*, 8302–8316; b) X. J. Kong, Y. P. Ren, L. S. Long, *Inorg. Chem.* **2008**, *47*, 2728–2739; c) H. M. Sommerfeldt, C. Meermann, K. W. Tornroos, *Inorg. Chem.* **2008**, *47*, 4696–4705.
[17] L. Li, H. T. Sheng, F. Xu, *Chin. J. Chem.* **2009**, *27*, 1127–1131.
[18] H. T. Sheng, J. M. Li, Y. Zhang, *J. Appl. Polym. Sci.* **2009**, *112*, 454–460.
[19] H. T. Sheng, J. M. Li, Y. Zhang, *Polyhedron* **2008**, *27*, 1665–1672.
[20] a) W. J. Evans, J. M. Olofson, J. W. Ziller, *J. Am. Chem. Soc.* **1990**, *112*, 2308; b) W. J. Evans, M. S. Sollberger, *Inorg. Chem.* **1988**, *27*, 4417.
[21] M. Mehring, S. Paalasmaa, M. Schurmann, *Eur. J. Inorg. Chem.* **2005**, 4891–4901.
[22] H. T. Sheng, F. Xu, Y. M. Yao, Y. Zhang, Q. Shen, *Inorg. Chem.* **2007**, *46*, 7722.

[23] J. B. Timothy, M. O. Leigh Anna, *Chem. Rev.* **2008**, *108*, 1896–1917.
[24] a) T. J. Boyle, L. A. M. Ottley, S. D. Daniel-Taylor, L. J. Tribby, S. D. Bunge, A. L. Costello, T. M. Alam, J. C. Gordon, M. McCleskey, *Inorg. Chem.* **2007**, *46*, 3705; b) T. J. Boyle, S. D. Bunge, P. G. Clem, J. Richardson, J. T. Dawley, L. A. M. Ottley, M. A. Rodriguez, B. A. Tuttle, G. Avilucea, R. G. Tissot, *Inorg. Chem.* **2005**, *44*, 1588; c) D. C. Bradley, H. Chudzynska, M. B. Hursthouse, M. Motevalli, *Polyhedron* **1991**, *10*, 1049.
[25] a) G. Westin, M. Moustiakimov, M. Kritikos, *Inorg. Chem.* **2002**, *41*, 3249; b) K. Yunlu, P. S. Gradeff, N. Edeletein, W. Kot, G. Shalimoff, W. E. Streib, K. G. Gaulton, *Inorg. Chem.* **1991**, *30*, 2317; c) M. Moustiakimov, M. Kritikos, G. Westin, *Inorg. Chem.* **2005**, *44*, 1499; d) W. J. Evans, M. A. Greci, J. W. Ziller, *Inorg. Chem.* **2000**, *39*, 3213.
[26] a) L. F. Sanchez-Barba, D. L. Hughes, S. M. Humphrey, M. Bochmann, *Organometallics* **2005**, *24*, 3792; b) M. Nishiura, Z. M. Hou, T. A. Koizumi, T. Imamoto, *Macromolecules* **1999**, *32*, 8245.
[27] S. J. MaLain, N. E. Drysdale, *US Patent*, **1991**, *5028*, 667.
[28] Y. M. Yao, X. P. Xu, B. Liu, Q. Shen, *Inorg. Chem.* **2005**, *44*, 5133.
[29] M. Yamashita, Y. Takemoto, E. Ihara, H. Yasuda, *Macromolecules* **1996**, *29*, 1798.
[30] H. T. Sheng, L. Y. Zhou, Y. Zhang, Y. M. Yao, Q. Shen, *J. Polym. Sci., Part A: Polym. Chem.* **2007**, *45*, 1210–1218.
[31] a) I. Saeed, S. Masashi, M. Toshio, *Macromolecules* **2006**, *39*, 5347–5351; b) B. Samuel, J. Owens, M. Gary, *Organometallics* **2008**, *27*, 4282–4287.
[32] G. M. Sheldrick, *SHELXL-97, Program for the Refinement of Crystal Structures*, University of Göttingen, Germany, **1997**.
Received: August 1, 2010
Published Online: November 5, 2010

